

1 **Rapid quantitative electrochemical detection of SARS-CoV-2 antibodies in**
2 **plasma and dried blood spot samples**

3

4 Sanjay S. Timilsina^{1,+}, Nolan Durr^{1,+}, Pawan Jolly¹, Donald E. Ingber^{1,2,3,*}

5 ¹*Wyss Institute for Biologically Inspired Engineering, Harvard University, 02115, USA,*

6 ²*Vascular Biology Program, Boston Children's Hospital, and Harvard Medical School, 02115, USA and*

7 ³*Harvard John A. Paulson School of Engineering and Applied Sciences, Harvard University, 02115, USA*

8 ⁺Current address: *StataDX Inc., Boston, MA 02215, USA*

9

10 *Address all correspondence to: Donald E. Ingber, MD, PhD., Wyss Institute at Harvard University,
11 CLSB5, 3 Blackfan Circle, Boston MA 02115 (ph: 617-432-7044, fax: 617-432-7828; email:

12 don.ingber@wyss.harvard.edu

13

14 **ABSTRACT**

15 **Coronavirus disease (COVID-19) caused by severe acute respiratory syndrome**
16 **coronavirus 2 (SARS-CoV-2), which is a highly contagious disease with several variants,**
17 **continues to spread as part of the global pandemic. With the roll-out of vaccines and**
18 **development of new therapeutics that may be targeted to distinct viral molecules, there is a**
19 **need to screen populations for viral antigen-specific SARS-CoV-2 antibodies. Here, we**
20 **describe a rapid, multiplexed, electrochemical (EC) platform with on-chip control that**
21 **enables detection of SARS-CoV-2 antibodies in less than 10 min using 1.5 μ L of a patient**
22 **sample. The EC biosensor demonstrated 100% sensitivity and specificity, and an area**
23 **under the receiver operating characteristic curve of 1, when evaluated using 93 clinical**
24 **samples, including plasma and dried blood spot samples from 54 SARS-CoV-2 positive and**
25 **39 negative patients. This EC biosensor platform enables simple, cost-effective, sensitive,**
26 **and rapid detection of anti-SARS-CoV-2 antibodies in complex clinical samples, which is**
27 **convenient for monitoring host humoral responses to vaccination or viral infection in broad**

1 **population testing, including applications in low-resource settings. We also demonstrate the**
2 **feasibility of using dried blood spot samples that can be collected locally and transported to**
3 **distant clinical laboratories at ambient temperature for detection of anti-SARS-CoV-2**
4 **antibodies which can be used for serological surveillance and demonstrate the utility of**
5 **remote sampling.**

6
7 **Key Words:** Electrochemical sensor, SARS-CoV-2 antibodies, serology, diagnostic, dried blood
8 spot.

9
10 **1. Introduction**

11 The global pandemic caused by severe acute respiratory syndrome coronavirus 2 (SARS-CoV-2)
12 has led to millions of infected individuals as well as global vaccination efforts.^[1] Real-time
13 reverse transcription-polymerase chain reaction (RT-PCR) and rapid antigen detection are used
14 to test for the presence of SARS-CoV-2 RNA and proteins in symptomatic and asymptomatic
15 individuals.^[2] While this was extremely critical in the early phase of the pandemic, serologic
16 testing of blood has become of greater interest more recently because it can detect the presence
17 of antibodies against specific SARS-CoV-2 virus proteins.^[3] This is important because this can
18 be used to assess whether patients had prior COVID-19 infection and determine the efficacy,
19 duration, and longevity of vaccine responses, as well as qualify convalescent plasma for
20 therapeutic purposes.^[4] Moreover, longitudinal evaluation of antibody titers in large populations
21 is essential to determine the strength and duration of immunity generated by exposure to the
22 primary virus, its variants, and vaccines, and all of this information is crucial for implementing
23 effective public policy and vaccination strategies.^[5]

24
25 Current SARS-CoV-2 vaccines induce the production of antibodies against SARS-CoV-2 Spike
26 (S) protein, but not against its nucleocapsid (N) protein, while natural infection produces
27 antibodies against both proteins, and thus diagnostic discrimination between these responses can
28 help to differentiate natural immunity from vaccine-induced immunity.^[6] Traditional serological
29 assays are not optimal for assessing antibody levels under pandemic conditions as enzyme-linked
30 immunosorbent assays (ELISAs) take several hours to complete due to the need for multiple

1 incubation and washing steps. Lateral flow immunoassays (LFIAs) are more rapid, but they
2 produce less reliable results and are qualitative rather than quantitative.^[7] Similarly, while Rapid
3 antigen detection tests (RADTs) now widely used in the United States for detection of viral
4 proteins could be adapted for detection of antibodies, they have low sensitivity.^[8] Another option
5 would be use of chemiluminescent enzyme immunoassays (CLIAs) (Abbott and Roche Elecsys),
6 however, they are expensive, lack scalability, and require specific integrated instrument
7 platforms.^[9] Many of these tests also must be carried out in a clinical research laboratory.
8 Guidelines implemented to prevent spread of viral infections such as SARS-CoV-2 during
9 serological surveillance also make collection of venous blood logistically difficult and have
10 generated interest in dried blood spot (DBS) sampling. This is because the blood can be self-
11 collected via a finger prick at-home or by community members and mailed to test sites at
12 ambient temperatures.^[10] Through their ease of storage and shipment, low cost, and minimally
13 invasive nature DBSs can be employed to screen large populations for antibody titers even in
14 low-resource settings. DBSs only require a few microliters of blood, can be easily multiplexed
15 and automated, and are compatible with a range of bioanalytical methods, namely
16 chromatography, spectroscopy, and immunoassays.^[11] Also, DBS do not require refrigeration for
17 shipment or storage and results obtained with these samples have been shown to correlate well
18 with those obtained from plasma or serum using ELISAs or commercial SARS-CoV-2 antigen
19 and antibody assays.^[12] DBS samples are also considered to be nonregulated and exempt
20 materials for shipping if they are properly packaged making it easy to return DBS specimens
21 from home directly to a clinical laboratory for testing.^[12b, 13] Thus, there is high demand for rapid
22 and cost-effective detection approaches to monitor levels of different SARS-CoV-2 antibodies to
23 assess patient responses infections and vaccines in a timely manner with high sensitivity and
24 specificity, which may be used either at the point-of-care (POC) or in clinical laboratories in
25 combination with use of DBS sampling.

26
27 Here, we describe an electrochemical (EC) biosensor platform that enables rapid, sensitive, and
28 highly specific detection of anti-SARS-CoV-2 antibodies from both plasma and DBS in minutes
29 (**Fig. 1**). The biosensor is coated with a previously reported antifouling nanocomposite coating
30 composed of bovine serum albumin (BSA) cross-linked with glutaraldehyde (GA) and doped
31 with highly conducting pentaamine-modified graphene nanoflakes (prGOx), which efficiently

1 prevents biofouling and reduces non-specific binding thereby greatly increasing assay sensitivity.
2 To develop a sensitive and specific serologic assay for COVID-19, specific ligands were
3 covalently immobilized on the coated EC sensor to capture SARS-CoV-2 antibodies. The EC
4 sensors also can be multiplexed to detect multiple different SARS-CoV-2 antibodies
5 simultaneously while also including on-chip controls. Analysis of plasma and DBS samples from
6 93 SARS-CoV-2 patients revealed that the EC sensor platform displayed 100% sensitivity and
7 100% specificity with Area under the ROC Curve (AUC) of 1 in less than 10 min using only 1.5
8 μL of sample.

9

10 **2. Methods**

11 **2.1 Fabrication of Electrochemical (EC) sensor**

12 EC sensor with gold electrodes purchased from Telic Company were custom fabricated using a
13 standard photolithography process. The gold sensor electrode chips were cleaned as described
14 previously.^[14] The BSA/prGOx/GA anti-fouling nanocomposite was prepared by mixing 8
15 mg/mL of prGOx (tetraethylene pentamine functionalized reduced graphene oxide) (Millipore
16 Sigma, no. 806579) with 5 mg/mL BSA (IgG-Free, Protease-Free, Bovine Serum Albumin)
17 (Jackson ImmunoResearch, no. 001-000-162) or Exbumin (Recombinant human albumin
18 excipient, InVitria, no. 777HSA097) in 10 mM phosphate-buffered saline solution (PBS, pH 7.4)
19 (Sigma Aldrich, USA, no. D8537). The solution was mixed using a vortex mixer and sonicated
20 in a tip sonicator for 30 min using 1 s on/off cycles at 50% amplitude, 125 W and 20 kHz
21 (Branson, CPX 3800), followed by heating (Labnet, no. D1200) at 105 °C for 5 min to denature
22 the protein. The mixture was kept at 4 °C until further use. Before applying antifouling
23 nanocomposite to the EC-sensor, the resulting opaque black mixture was centrifuged at 16.1
24 relative centrifugal force for 15 min to remove the excess aggregates. The semi-transparent
25 nanocomposite supernatant solution was then mixed with 70% glutaraldehyde (Sigma Aldrich,
26 USA, no. G7776) for crosslinking in the ratio of 70:2. Cleaned and plasma-treated (0.5 mbar and
27 50% power for 8 min) sensors were kept over a hot plate for 2 min for the temperature to
28 equilibrate to 85 °C. 70 μL of anti-fouling nanocomposite was then drop cast to each chip and
29 incubated for 45s.^[15] The sensors were immediately washed by dipping in PBS, rinsed at 400
30 rpm for 10 min, and dried with a slide spinner (Millipore Sigma, no. 674664).

31

1 **2.2 Detection of SARS-CoV-2 IgG in EC-Biosensor and ELISA**

2 1-ethyl-3-(3-dimethyl aminopropyl) carbodiimide hydrochloride (EDC, Thermo Fisher
3 Scientific, no. 22980) and N-hydroxysuccinimide (NHS, Sigma Aldrich, no. 130672) were used
4 to conjugate the capture protein to the surface of the sensor with antifouling nanocomposite.
5 Briefly, EDC (400 mM) and NHS (200 mM) were dissolved in 50 mM MES (2-(N-morpholino)
6 ethanesulfonic acid) buffer (pH 6.2) and deposited on the gold sensor electrodes with antifouling
7 nanocomposite for 30 min at room temperature in the dark for surface activation. Sensors were
8 then quickly rinsed with Milli Q water and dried with compressed air before spotting of capture
9 protein (0.6 mg/mL) on top of the three working electrode areas using Xtend capillary
10 microarray Pin (LabNEXT, no. 007-350). The fourth working electrode was always spotted with
11 5 mg/mL BSA/recombinant Human Albumin (rHA) (InVitria, no. 777HSA097) as a negative
12 control and stored overnight at 4 °C in a humidity chamber. After conjugation, biosensors were
13 washed with PBS and quenched with 15 µL of 1M ethanolamine (SigmaAldrich, no. E9508) for
14 30 min and blocked with 10 µL of 2.5% BSA/rHA in PBS for 1 hour.

15 Detection of anti-SARS-CoV-2 IgG was performed on the biosensor using the optimized
16 conditions. Three working electrodes were spotted with a capture N protein (SARS-CoV-2
17 Nucleocapsid protein (His Tag), GenScript, no. Z03480) diluted in PBS (0.6 mg/mL). SARS-
18 CoV-2 positive or negative plasma samples were diluted 10-fold using 1 % BSA/rHA in PBS.
19 Mouse monoclonal anti-Human IgG Fc (abcam, no. ab99759) linked with HRP (horseradish
20 peroxidase) was diluted to 40 µg/mL in 1 % BSA/rHA in PBS. Diluted clinical samples were
21 mixed with detection antibody in the ratio of 9:1 and 15 µL was added to each biosensor and
22 incubated for seven minutes. Biosensors were then washed with PBST (PBS with 0.05 % Tween
23 20 (Sigma Aldrich, no. P9416)). 10 µL of precipitating 3,3',5,5'-Tetramethylbenzidine (TMB,
24 Sigma-Aldrich, USA, no. T9455) was then added to biosensors and incubated for 1 min before
25 washing. Finally, measurement was performed in 10 µL of PBST using a potentiostat (Autolab
26 PGSTAT128N, Metrohm) by cycling the potential between -0.5 and 0.5 V with a scan rate of 1
27 V/s vs. on-chip integrated gold quasi-reference electrode. Peak height was then calculated using
28 Nova 1.11 software for data analysis.

29 For standard ELISA of the biomarkers, 100 µL of 1 µg/mL capture N protein in carbonate-
30 bicarbonate buffer at pH 9.2 was added to Nunc™ MaxiSorp™ ELISA plates (BioLegend, no.

1 423501) and incubated overnight at 4 °C. The plates were washed 3 times with 200 µL of PBST
2 followed by the addition of 200 µL of 5% Blotto (Fisher Scientific, no. NC9544655) for 1h.
3 After washing the plates, 100 µL of 200-fold diluted clinical plasma samples were added and
4 incubated for 30 min. After rewashing the plates, 100 µL of 50 ng/mL of horseradish peroxidase
5 (HRP)-linked detection antibody was added for 30 min. The plate was then washed and 150 µL
6 of turbo TMB (Thermo Scientific, no. 34022) was added for 20 min, followed by 150 µL of Stop
7 solution to stop the reaction. The plate was immediately read using a microplate reader at 450
8 nm. All clinical samples were collected under the approval of the Institutional Review Board for
9 Harvard Human Research Protection Program (IRB21-0024).

10

11 **2.3 Screening of detection antibody and capture Nucleocapsid (N) protein**

12 For screening of detection antibody, N protein from Raybiotech was immobilized on EC-
13 biosensor and ELISA. For ELISA, 8 positive and 8 negative and for EC-biosensor, 4 positive and
14 2 negative SARS-CoV-2 samples were tested. Six screened detection antibodies include Goat
15 anti-Human IgG Fc Secondary Antibody, HRP (ThermoFisher Scientific, no. A18817); Goat
16 anti-Human IgG (Fc specific)–Peroxidase (Millipore Sigma, no. A0170); Peroxidase AffiniPure
17 F(ab')₂ Fragment Goat anti-Human IgG, Fcγ (Jackson ImmunoResearch, no. 109-036-170);
18 Mouse monoclonal anti-Human IgG Fc-HRP (abcam, no. ab99759); Human IgG-Fc Fragment
19 Antibody (Bethyl Laboratories, no. A80-148P); and AffiniPure Goat anti-human IgG, Fc
20 fragment specific (Jackson ImmunoResearch, no. 109-005-008). Similarly, for screening of
21 capture N protein 8 positive and 6 negative (ELISA) and 7 positive and 5 negative (EC-
22 biosensor) SARS-CoV-2 samples were tested. 5 different N proteins screened include, SARS-
23 CoV-2 Nucleocapsid protein (GenScript, no. Z03480); Recombinant SARS-CoV-2 Nucleocapsid
24 Protein (RayBiotech, no. 230-30164); SARS-CoV-2 Nucleocapsid (AA 1-419) protein
25 (antibodies-online, no. ABIN6952315); SARS-CoV-2 Nucleocapsid-His recombinant Protein
26 (SinoBiological, no. 40588-V08B); and SARS-CoV-2 Nucleoprotein, His-Tag (NativeAntigen
27 no. REC31851).

28

29 **2.4 Assay Development and optimization**

30 Sandwich ELISA was performed both on EC-sensor and ELISA. Initially, a feasibility study was
31 performed where a biotin-labeled detection antibody followed by the addition of Poly-HRP-

1 Streptavidin (Thermo Fisher Scientific, no. N200) was replaced by HRP labeled detection
2 antibody to reduce the assay steps and complexity. The assay was performed on both ELISA and
3 EC-sensor with 2 positive, 2 negative, and blotto as a negative control. An assay for the
4 optimization of the concentration of detection antibody was then performed on EC-biosensor. 4
5 positive and 3 negative SARS-CoV-2 samples were tested with different concentrations of
6 detection antibody ranging from 5-80 $\mu\text{g/mL}$. Likewise, optimization of the concentration of
7 capture N protein from 0.1-0.9 $\mu\text{g/mL}$ was performed using 2 positive and 3 negative SARS-
8 CoV-2 samples.
9 Similarly, the optimum sample dilution study was performed using undiluted and diluted
10 samples (5 - 15-fold in 1% BSA/rHA) with 3 positive and 2 negative SARS-CoV-2 samples.
11 Finally, the optimum assay time was studied where different incubation time of the sample (7-12
12 min) was performed against TMB incubation time of 1 and 2 min. Furthermore, a titration study
13 was carried out to validate the clinical sample dilution and incubation timing. Three high titer
14 positive samples and two negative samples were taken for the titration study and clinical samples
15 were diluted from 0 - 1000-fold before performing the assay. In addition, a study was performed
16 to compare the effectiveness of rHA over BSA. The assay was performed with 5 positive and 4
17 negative SARS-CoV-2 samples along with BSA/rHA as a negative control. To overcome the
18 regulatory hurdle of using BSA in a medical device, nanocomposite coating was prepared with
19 BSA and rHA, which was evaluated by performing the whole EC assay. Briefly, the coating was
20 prepared by replacing BSA with rHA followed by functionalization with 0.6 mg/mL N protein or
21 5mg/mL BSA/rHA as a negative control. Then, the chips were blocked with 15 μL of
22 ethanolamine followed by 10 μL of 2.5% BSA/rHA and used the respective buffer to run 10-fold
23 diluted SARS-CoV-2 samples (5 positive and 4 negative).

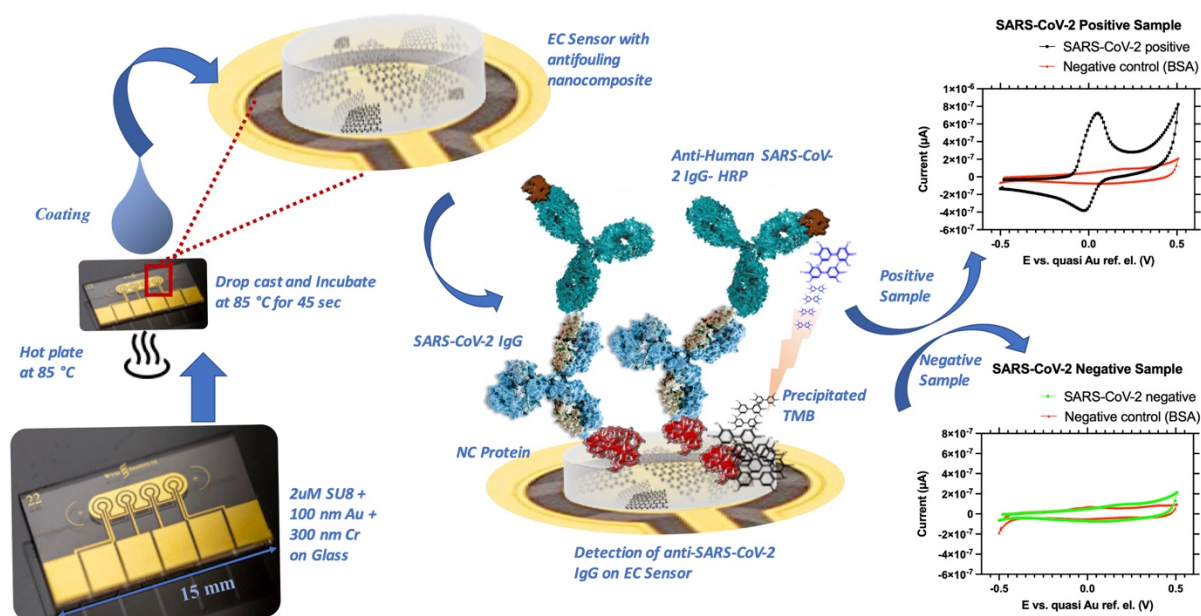
24

25 **2.5 Anti-SARS-CoV-2 IgG detection on EC-sensor using Clinical samples.**

26 Optimized assay conditions were used to run clinical samples on EC sensors. 23 SARS-CoV-2
27 positive and 21 SARS-CoV-2 negative clinical samples were purchased from Ray Biotech and
28 BWH Crimson Core Laboratory and kept at -80 $^{\circ}\text{C}$ until further use. An additional 23 positive
29 and 14 negative SARS-CoV-2 samples were purchased from National Institute for Biological
30 Standards and Control (NIBSC). Similarly, 8 SARS-CoV-2 positive and 4 SARS-CoV-2
31 negative Dried Blood Spots on Whatman filter paper #903 were purchased from RayBiotech

1 (CoV-DBS-1) and kept at -80°C until further use. For reconstitution of DBS, Whatman filter
2 paper with dried blood was kept in a tube and $300\ \mu\text{L}$ of 0.05% PBST was added and kept on a
3 shaker overnight. The reconstituted DBS was then directly used for the assay of anti-SARS-
4 CoV-2 IgG. A time-point study of SARS-CoV-2 was also carried out to understand
5 seroconversion better. Plasma samples were collected on 5 different days (10-21) after the onset
6 of symptoms of COVID-19 for each person. The study was performed with 3 different patients.
7 To run anti-N SARS-CoV-2 Rabbit IgG assay, we immobilized the EC sensor with $0.6\ \text{mg/mL}$ N
8 protein or $5\ \text{mg/mL}$ rHA as a negative control. After blocking the chip, $15\ \mu\text{L}$ of different
9 concentrations of SARS-CoV-2 rabbit IgG samples were spiked to pre-pandemic plasma samples
10 and incubated on the chip for 30 min. Then, the chips were washed and $10\ \mu\text{L}$ of 1:1000 Anti-
11 rabbit IgG-HRP (RayBiotech, no. 130-10760-100) prepared in 1% rHA was added to the chip for
12 10 min. Chips were washed, and finally, precipitating TMB was added for 1 min before washing
13 and EC measurement. For the calibration curve of NIBSC diagnostic calibrant, the assay was run
14 using the optimized condition in 1% rHA and pre-pandemic plasma sample.

15



16

17

18 **Figure 1.** Schematic of the multiplexed EC sensor platform. The antifouling nanocomposite is
19 rapidly drop cast on the gold electrodes of the EC sensor (left). A sandwich assay was used
20 to measure SARS-CoV-2 IgG bound to Nucleocapsid (NC Protein) that was pre-immobilized on the
21 nanocomposite coating above sensor where TMB precipitates to generate an EC signal (middle).

1 *The top and bottom graphs represent CV for positive and negative SARS-CoV-2 samples,*
2 *respectively, with on-chip negative control.*

3

4 **3. Results**

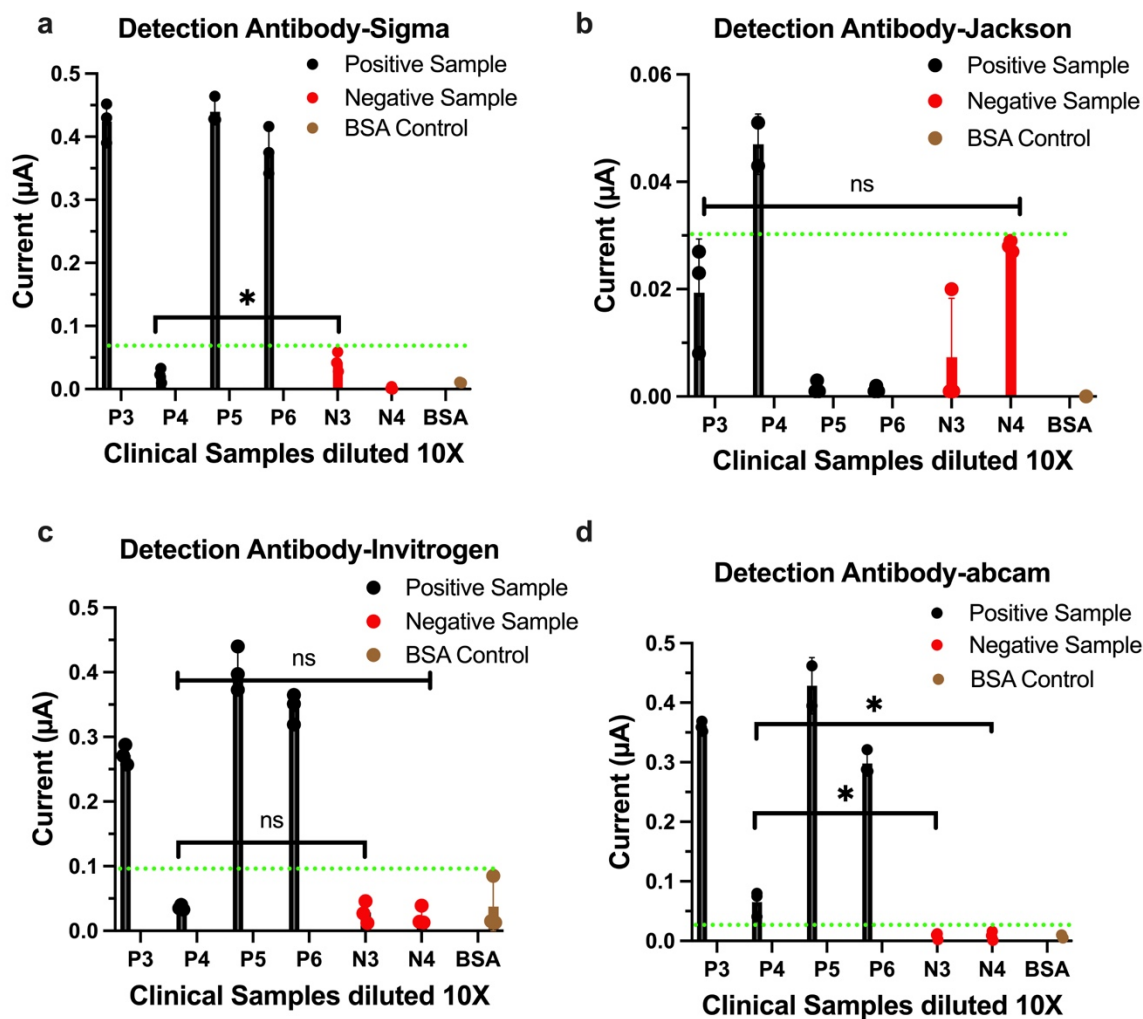
5 **3.1 Single-Step Assay Development**

6 A sandwich ELISA was performed using the EC sensor and an ELISA during assay
7 development. An initial feasibility study was performed where a biotin-labeled detection
8 antibody (followed by washing and addition of streptavidin-polyHRP) was replaced by HRP-
9 labeled detection antibody (single-step assay) to reduce the assay steps and complexity. Using
10 traditional ELISA, with both biotin and HRP-labeled detection antibody, a significantly higher
11 signal for positive samples was observed compared to negative SARS-CoV-2 samples for both
12 the viral N and S proteins (**Fig. S1a,b**). However, on the EC platform, the HRP-labeled detection
13 antibody showed a higher signal for positive samples and no signal for negative samples as
14 compared to the EC assay with biotin detection antibody where a small signal for 1 negative
15 sample was observed (**Fig S1c,d**). Thus, the HRP-linked detection antibody was used for further
16 experiments because it significantly reduces complexity and assay time without compromising
17 assay sensitivity. After the feasibility of the HRP-labeled detection antibody was established, the
18 anti-SARS-CoV-2 IgG detection antibody concentration was varied from 5- 80 µg/mL to
19 establish a single-step assay (**Fig. S2**). The concentration-dependent increases in positive signals
20 were observed and 40 µg/mL of detection antibody was determined to be the optimum
21 concentration, which was used in all further experiments.

22 **3.2 Screening of detection antibodies for capture of N protein**

23 Studies have shown that the sensitivity and specificity for the serological assay of SARS-CoV-2
24 antibody is significantly affected by choice of capture antigen and detection antibody (human
25 anti-SARS-CoV-2).^[16] We screened six commercially available SARS-CoV-2 IgG detection
26 antibodies to find the antibody with the highest sensitivity and specificity for the EC platform.
27 Using ELISA, all the detection antibodies showed a similar pattern for positive and negative
28 samples, where up to 25% of positive samples displayed lower signals than one of the negative
29 samples. However, the Sigma and Abcam detection antibodies had comparatively lower signals
30 for negative controls (**Fig. S3**). When the EC biosensor was used, detection antibodies obtained
31 from Sigma (**Fig. 2a**), Jackson (**Fig. 2b**), and Invitrogen (**Fig. 2c**) could not clearly differentiate

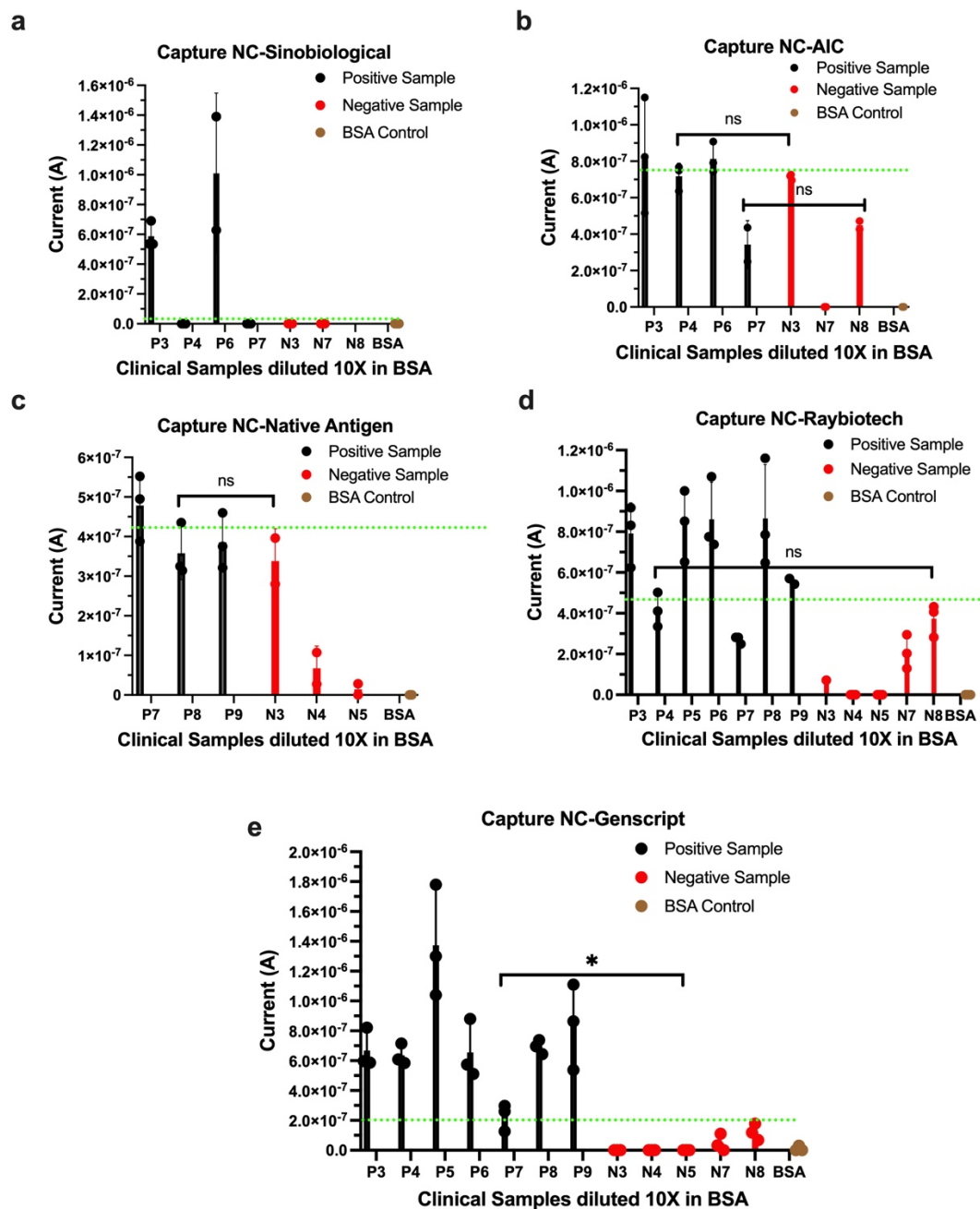
1 between positive and negative samples. However, with Abcam detection antibody, even the low
 2 titer positive sample gave a significantly higher signal than negative samples (Fig. 2d). Thus, as
 3 the Abcam detection antibody could differentiate all positive and negative samples, it was used
 4 for further experiments to obtain a highly sensitive and specific assay.



5
 6 **Figure 2.** Screening of anti-human SARS-CoV-2 IgG detection antibody on EC-biosensor from
 7 four commercial sources, including Sigma (a), Jackson ImmunoResearch (b), abcam (c), and
 8 Invitrogen (d). Error bars represent the s.d. of the mean; n=3; P= SARS-CoV-2 positive sample;
 9 N=SARS-CoV-2 negative sample; and BSA=Negative Control. Green dotted line represents
 10 highest signal for negative sample/control. Statistical analysis was performed by unpaired t-test
 11 (ns $P > 0.05$; * $P < 0.05$); all two-tailed.

12

1 All viral proteins elicit antibody responses to some extent, but it is necessary to identify proteins
2 to which the immune system best responds and produces the highest affinity antibodies to
3 increase the sensitivity and specificity of a serological assay. Moreover, the more unique the
4 protein is, the lower the cross-reactivity with other coronaviruses.^[17] Thus, we then screened
5 various sources of N protein for their ability to be detected by the Abcam antibody. When tested
6 by ELISA, use of the Genescript N protein resulted in one negative sample showing a similar
7 signal as a positive sample and when N protein from Sinobiological and AIC was used, some
8 positive samples showed lower signals than negative one (**Fig. S4b,c**). With other N capture
9 proteins, 3 or more positive samples showed lower signals than some negative samples (**Fig. S4**).
10 When we screened N proteins in the EC biosensor, the N protein from Sinobiological (**Fig. 3a**),
11 AIC (**Fig. 3b**), Native Antigen Company (**Fig. 3c**) produced aberrant signals that did not scale
12 with positive or negative samples. Finally, N capture protein obtained from Raybiotech and
13 Genscript both generated signals for all positive samples, however, the Genscript protein had
14 lower signals in the negative samples (**Fig. 3d,e**). Thus, Genscript N protein was used for further
15 experiments because it showed high sensitivity and specificity and could differentiate all positive
16 and negative controls.



1
 2 **Figure 3.** Screening of SARS-CoV-2 N capture protein on EC-biosensor from five commercial
 3 sources, including Raybiotech (a), Sinobiological (b), Advanced ImmunoChemical (c), Native
 4 Antigen Company (d), and Genscript (e). Error bars represent the s.d. of the mean; n=3; P=
 5 SARS-CoV-2 positive sample; N=SARS-CoV-2 negative sample; and BSA=Negative Control.
 6 Green dotted line represents highest signal for negative sample/control. Statistical analysis was
 7 performed by unpaired t-test (ns $P > 0.05$; * $P < 0.05$); all two-tailed. Green dotted line
 8 represents signal for negative sample with the highest value.

1 **3.3 Assay optimization**

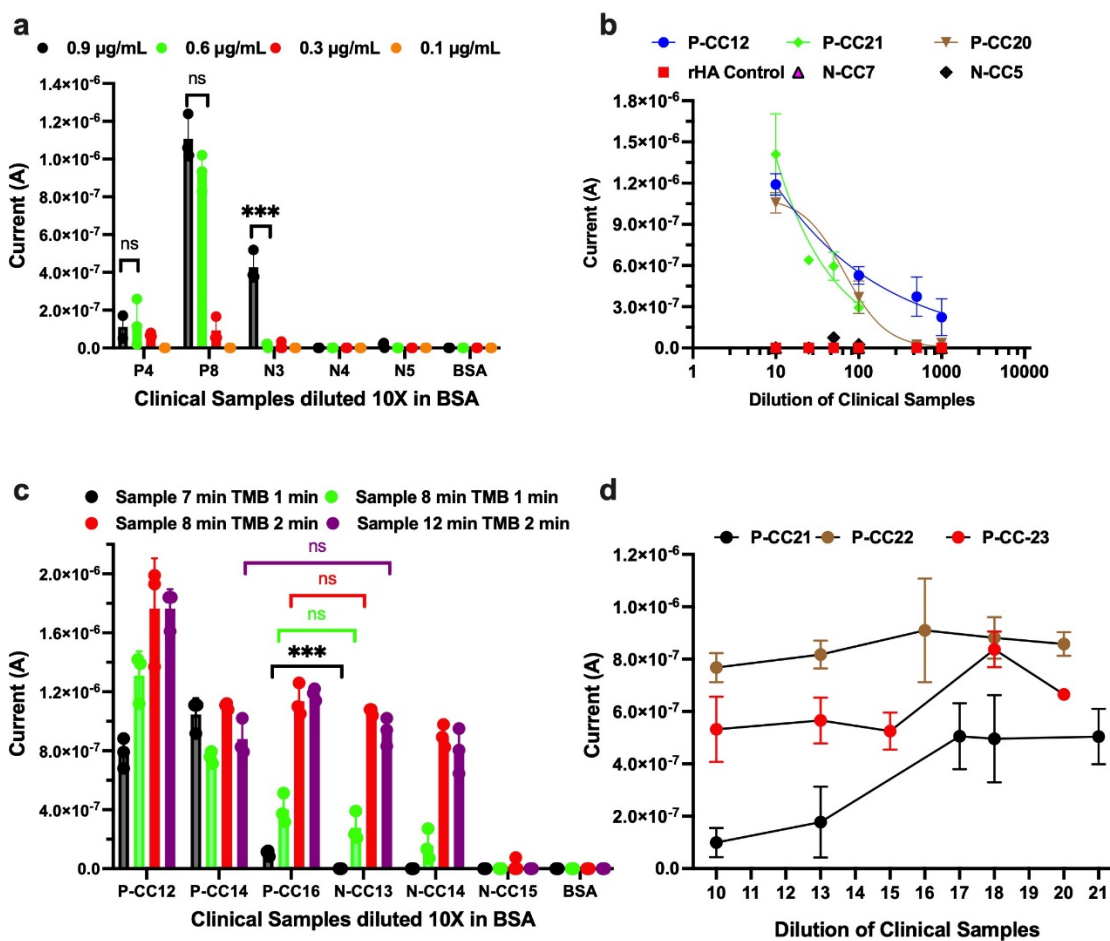
2 The coating density of N protein on the electrode surface is critical to achieve the optimal
3 surface-to-volume ratio necessary for efficiently capturing and detecting anti-SARS-CoV-2 IgG
4 in the test sample. Thus, to reduce non-specific binding and increase assay sensitivity, we
5 examined the effect of varying N protein concentration (from 0.1 to 0.9 $\mu\text{g/mL}$). These studies
6 revealed the optimum concentration of capture N protein to be 0.6 $\mu\text{g/mL}$ (**Fig. 4a**).

7
8 To avoid the hook and matrix effect, we studied the effect of sample dilution (0 to 15-fold) for
9 the detection of anti-SARS-CoV-2 IgG. In general, an increase in signal was observed with
10 positive samples from undiluted to 5- and 10-fold dilution, saturating at 10- to 15-fold (**Fig.**
11 **S5a**). Thus 10-fold dilution was considered optimum because below this level of dilution the
12 signal was suppressed, likely due to combined hook and matrix effect.

13
14 To better understand the dilution required and the feasibility of rapid testing as a quantitative
15 method, a titration study was performed where high titer anti-SARS-CoV-2 IgG clinical samples
16 were serially diluted from 0 to 1000-fold (**Fig. 4b** and **Fig. S5b**). Signal generated with positive
17 samples increased with 0- to 10-fold dilution, possibly due to the hook's effect. As expected, the
18 negative samples did not show any signal, and the signal for all positive samples decreased
19 proportionally to the increase in dilution from 10- to 1000-fold. Thus, the titration study also
20 revealed that a 10-fold dilution of the sample is optimal for the study.

21
22 To perform rapid detection of anti-SARS-CoV-2 IgG with high sensitivity and specificity, we
23 also optimized the sample incubation time and TMB concentration. With sample incubation time
24 of 7 min and TMB time of 1 min (black bar), all the positive samples showed signals while all
25 negative samples did not (**Fig. 4c**). When sample incubation time was increased to 8 or 12 min
26 with a TMB time of 1 or 2 min, we lost the ability to discriminate between some positive and
27 negative samples. Thus, a sample incubation time of 7 min and TMB precipitation time of 1 min
28 was considered to the optimum. In addition, to understand the seroconversion, we performed a
29 time point study using an anti-SARS-CoV-2 IgG clinical sample in the three patient groups. As
30 expected, the levels of anti-SARS-CoV-2 IgG generally increased over the first 17 days from the
31 onset of symptoms which is consistent with previous reports (**Fig. 4d**).^[18]

1 We also performed an assay to observe if BSA in the antifouling coating and the blocking buffer
 2 could be replaced by recombinant human albumin (rHA) without compromising sensitivity and
 3 specificity of the assay. We explored rHA as it is blood and animal component-free recombinant
 4 human albumin excipient which is U.S. Food and Drug Administration (FDA) and (European
 5 Medicines Agency) EMA-approved excipient.^[19] rHA Both BSA and rHA-based coating
 6 produced similar signals for all positive samples, however, there was less signal in the negative
 7 samples using rHA (Fig. S6).



8
 9 **Figure 4.** Assay development and optimization on EC-sensor for detection of SARS-CoV-2 IgG.
 10 (a) Optimization of concentration of capture N protein. (b) Titration of high titer SARS-CoV-2
 11 positive clinical samples. (c) Optimization of sample and TMB incubation time for rapid
 12 detection of SARS-CoV-2 IgG. (d) Time-point study of anti-SARS-CoV-2 IgG clinical sample
 13 from 10-21 days after the onset of symptoms. Error bars represent the s.d. of the mean; n=3; P
 14 and P-CC= SARS-CoV-2 positive sample; N and N-CC=SARS-CoV-2 negative sample; and

1 *BSA=Negative Control. Statistical analysis was performed by unpaired t-test (ns $P > 0.05$;*
2 ** $P < 0.05$; ** $P < 0.01$; *** $P < 0.001$); all two-tailed.*

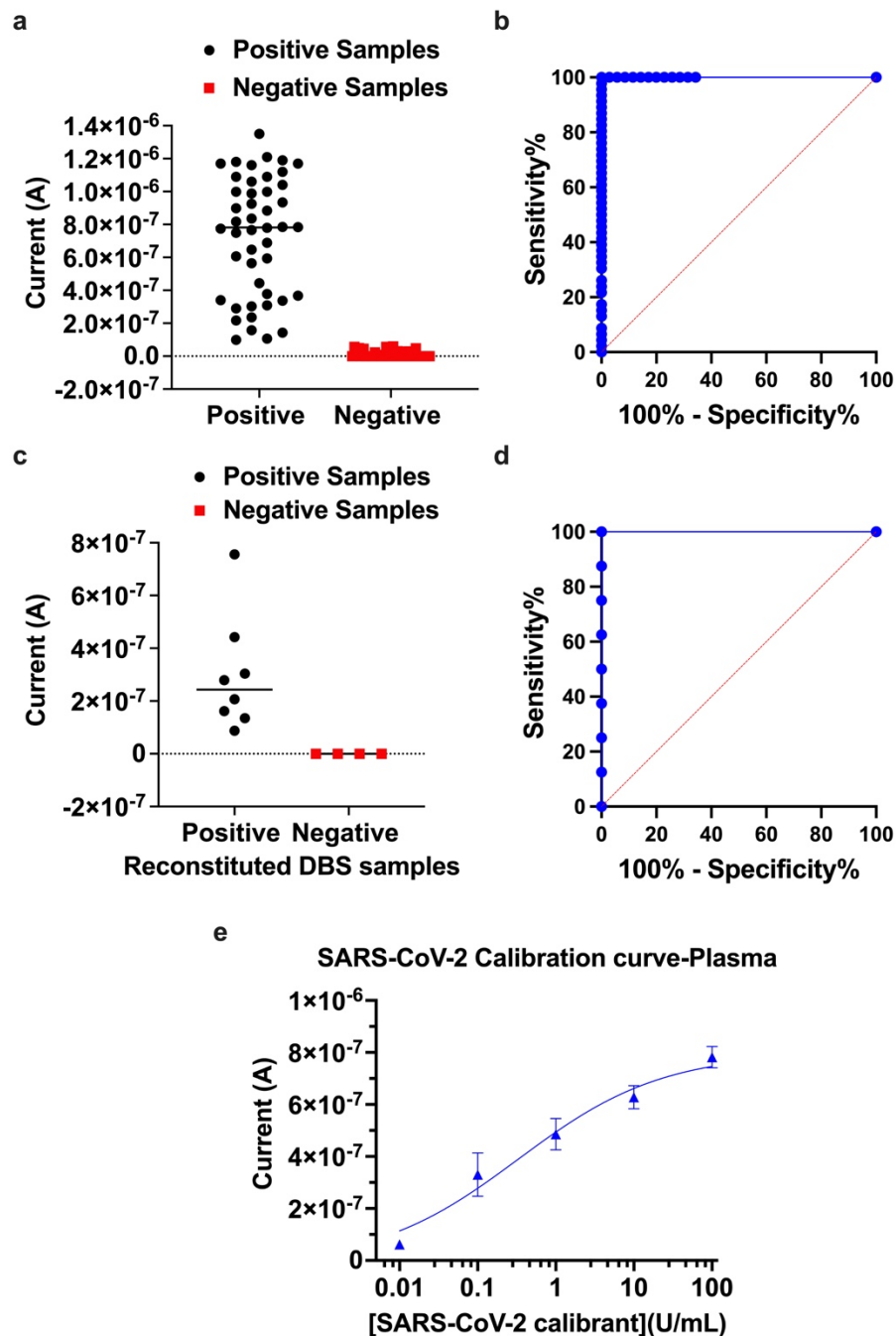
3

4 **3.4 Validation of EC-Biosensor using Clinical Samples**

5

6 We then used the EC sensor to test 46 positive and 35 negative SARS-CoV-2 clinical plasma
7 samples to validate its usefulness. These studies revealed that all negative samples showed
8 minimum or no signal and all the positive samples showed a significantly higher signal (**Fig. 5a**).
9 Analysis of the ROC curve revealed that the assay displayed 100% sensitivity and 100%
10 specificity with AUC=1 (**Fig. 5b**). We then carried out the same assay using 12 DBS samples,
11 which confirmed that the EC sensor can be used to detect IgG in reconstituted dried blood
12 without any further treatment. All positive DBS samples showed signal while none of the
13 negative samples did, which again shows 100% sensitivity and specificity (**Fig. 5 c,d**). The high
14 sensitivity and specificity of the EC sensor may be attributed to the highly efficient antifouling
15 BSA/prGOx/GA coating, which has very low non-specific binding and allow us to perform the
16 assay in plasma with minimum matrix effect. For a proof-of-concept quantitative assay, the anti-
17 N SARS-CoV-2 rabbit IgG calibration curve was run on the EC sensor and we detected a
18 sensitivity of 1 ng/mL (**Fig. S7a**).

19 The clinical utility of the quantitative detection of SARS-CoV-2 antibody using the EC sensor
20 was further validated by generating a calibration curve using the NIBSC anti-SARS-CoV-2
21 antibody diagnostic calibrant. Initially, a calibration curve was run with 1% rHA in PBS (**Fig.**
22 **S7b**). However, after successful detection of the anti-SARS-CoV-2 antibody diagnostic calibrant
23 in buffer, a pre-pandemic plasma sample without anti-SARS-CoV-2 IgG was used to run the
24 calibration curve, which demonstrated a sensitivity of 0.01 U/mL (**Fig. 5e**).



1

2 **Figure 5.** Clinical validation of EC-sensor for detection of SARS-CoV-2 IgG. Scattered graph
 3 (a) and ROC curve (b) for detection of 46 positive and 35 negative SARS-CoV-2 clinical plasma
 4 samples. Scattered graph (c) and ROC curve (d) for detection of 8 positive and 4 negative SARS-
 5 CoV-2 clinical Dried Blood Spot. (e) Calibration curve using NIBSC Anti-SARS-CoV-2 antibody
 6 diagnostic calibrant using pre-pandemic plasma sample. Error bars represent the s.d. of the
 7 mean; $n = 3$. Analysis was done using 4-Parameter Logistic (4PL) curve fitting.

1 **4. Conclusion and Discussion**

2 In this study, we developed and validated a rapid multiplexed EC detection platform for
3 monitoring COVID-19 and vaccination status by detecting SARS-CoV-2 antibodies with 100%
4 sensitivity and specificity. The antifouling coating, we utilized increases the conductivity of the
5 EC sensor and decreases nonspecific binding, which minimizes the EC background, hence
6 increasing the sensitivity and selectivity of the assay. This EC sensor also can be used for rapid
7 quantitative detection of SARS-CoV-2 IgG using just 1.5 μ L of plasma sample within 10 min
8 with 100% sensitivity and specificity. The potential of the EC-biosensor to perform assay with
9 DBS was also demonstrated using clinical DBS samples with 100% sensitivity and specificity
10 which can be used for serological surveillance utilizing remote sampling and shipment without
11 refrigeration. In addition, validation of the quantitative capability of the EC-sensor was carried
12 out by performing the calibration curve of a NIBSC SARS-CoV-2 calibrant in buffer and pre-
13 pandemic plasma samples. Thus, these studies demonstrate the potential value of this antifouling
14 EC-biosensor with its high sensitivity and selectivity for rapid quantitative detection of
15 biomarkers in serologic assays that can be carried out in a multiplexed fashion, potentially at the
16 point-of-care.

17 Antibody titers can remain stable over several months and extensive cohort studies in
18 hospitalized patients show that IgG antibodies against viral proteins correlate with disease
19 severity and outcome. In addition, rapid seroprevalence studies can differentiate reinfections
20 versus breakthrough infections to better understand herd immunity and vaccine efficacy in the
21 context of a pandemic, which is critical for the decision to reopen economies.^[6, 20] Hence, this
22 type of serological assay could be used to provide critical information to respond to epidemics or
23 pandemics, manage patient care and public health strategies, assess patient responses to
24 vaccination, and help determine when and if boosters might be required.^[21]

25

26 **Statistical Analysis**

27 ELISA reading is reported as absorbance (a.u.) of the mean of replicates and error bars
28 represent the standard deviation (s.d.) of the mean; $n = 2$. For EC-biosensor studies, peak heights
29 were calculated using Nova 1.11 software. Error bars represent mean \pm s.d. for all EC-biosensor

1 studies (sample sizes and statistical tests used are indicated in the Figure legends). All data was
2 plotted, and statistical tests were performed using GraphPad Prism 8, and 4-Parameter Logistic
3 (4PL) curve fitting was done for calibration curve analysis.

4

5 **Supporting Information**

6 Supporting Information includes single step assay development, optimization of detection
7 antibody concentration, screening of capture and detection antibody using ELISA, optimization
8 of sample dilution, titration of high titer SARS-CoV-2 positive samples, BSA vs rHA
9 characterization, and calibration curve of SARS-CoV-2 IgG.

10

11 **Data availability**

12 The main data supporting the results in this study are available within the paper and its
13 Supplementary Information. All raw and processed images/data generated in this work, including
14 the representative images provided in the manuscript, are available from the corresponding
15 authors on reasonable request.

16

17 **Acknowledgments**

18 We acknowledge research funding from the Wyss Institute for Biologically Inspired Engineering
19 at Harvard University and GBS Inc.

20

21 **Conflict of Interests**

22 This technology has been licensed to StataDX Inc. for neurological and kidney disease
23 diagnostics; P.J. and D.E.I. hold equity in StataDx and D.E.I. is a board member; S.S.T., N.D.,
24 P.J., and D.E.I are also listed as inventors on patents describing this technology.

25

1 REFERENCES

- 2 [1] C. T. Turgeon, K. A. Sanders, D. Granger, S. L. Nett, H. Hilgart, D. Matern, E. S. Theel, *Diagnostic*
3 *microbiology and infectious disease* **2021**, 101, 115425.
- 4 [2] a) Y. Rasmi, X. Li, J. Khan, T. Ozer, J. R. Choi, *Analytical and bioanalytical chemistry* **2021**, 1; b) S.
5 Mavrikou, G. Moschopoulou, V. Tsekouras, S. Kintzios, *Sensors* **2020**, 20, 3121.
- 6 [3] a) A. Yakoh, U. Pimpitak, S. Rengpipat, N. Hirankarn, O. Chailapakul, S. Chaiyo, *Biosensors and*
7 *Bioelectronics* **2021**, 176, 112912; b) E. Morales-Narváez, C. Dincer, *Biosensors and*
8 *Bioelectronics* **2020**, 163, 112274.
- 9 [4] a) R. West, A. Kobokovich, N. Connell, G. K. Gronvall, *Trends in Microbiology* **2021**, 29, 214; b) D.
10 Najjar, J. Rainbow, S. Sharma Timilsina, P. Jolly, H. De Puig, M. Yafia, N. Durr, H. Sallum, G. Alter,
11 J. Z. Li, *Nature biomedical engineering* **2022**, 6, 968.
- 12 [5] a) S. K. Elledge, X. X. Zhou, J. R. Byrnes, A. J. Martinko, I. Lui, K. Pance, S. A. Lim, J. E. Glasgow, A.
13 A. Glasgow, K. Turcios, *Nature Biotechnology* **2021**, 1; b) M. Jeyanathan, S. Afkhami, F. Smaill, M.
14 S. Miller, B. D. Lichty, Z. Xing, *Nature Reviews Immunology* **2020**, 20, 615; c) J. Seow, C. Graham,
15 B. Merrick, S. Acors, S. Pickering, K. J. Steel, O. Hemmings, A. O’Byrne, N. Kouphou, R. P. Galao,
16 *Nature microbiology* **2020**, 5, 1598.
- 17 [6] S. Gazit, R. Shlezinger, G. Perez, R. Lotan, A. Peretz, A. Ben-Tov, D. Cohen, K. Muhsen, G.
18 Chodick, T. Patalon, *MedRxiv* **2021**.
- 19 [7] a) B. Flower, J. C. Brown, B. Simmons, M. Moshe, R. Frise, R. Penn, R. Kugathasan, C. Petersen, A.
20 Daunt, D. Ashby, *Thorax* **2020**, 75, 1082; b) M. Michel, A. Bouam, S. Edouard, F. Fenollar, F. Di
21 Pinto, J.-L. Mège, M. Drancourt, J. Vitte, *Frontiers in microbiology* **2020**, 11.
- 22 [8] a) S. Kanjilal, S. Chalise, A. S. Shah, C.-A. Cheng, Y. Senussi, R. Uddin, V. Thiriveedhi, H. E. Cho, S.
23 Carroll, J. Lemieux, S. Turbett, D. R. Walt, *medRxiv* **2022**, DOI:
24 10.1101/2022.02.17.222711422022.02.17.22271142; b) S. Kanjilal, S. Chalise, A. S. Shah, C.-A.
25 Cheng, Y. Senussi, M. Springer, D. R. Walt, *medRxiv* **2022**.
- 26 [9] S. S. Tan, S. Saw, K. L. Chew, C. Wang, A. Pajarillaga, C. Khoo, W. Wang, Z. M. Ali, Z. Yang, Y. H.
27 Chan, *Archives of pathology & laboratory medicine* **2021**, 145, 32.
- 28 [10] M. P. Wong, M. A. Meas, C. Adams, S. Hernandez, V. Green, M. Montoya, B. M. Hirsch, M.
29 Horton, H. L. Quach, D. L. Quach, *Microbiology spectrum* **2022**, 10, e02471.
- 30 [11] P. A. Demirev, *Analytical chemistry* **2013**, 85, 779.
- 31 [12] a) F. Amini, E. Auma, Y. Hsia, S. Bilton, T. Hall, L. Ramkhelawon, P. T. Heath, K. Le Doare, *PLoS*
32 *One* **2021**, 16, e0248218; b) T. T. Zava, D. T. Zava, *Bioanalysis* **2021**, 13, 13.
- 33 [13] C. f. D. Control, Prevention, *Updated October* **2017**, 24.
- 34 [14] J. S. Del Río, O. Y. Henry, P. Jolly, D. E. Ingber, *Nature nanotechnology* **2019**, 14, 1143.
- 35 [15] a) S. S. Timilsina, P. Jolly, N. Durr, M. Yafia, D. E. Ingber, *Accounts of Chemical Research* **2021**, 54,
36 3529; b) S. S. Timilsina, M. Ramasamy, N. Durr, R. Ahmad, P. Jolly, D. E. Ingber, *Advanced*
37 *Healthcare Materials* **2022**, 2200589.
- 38 [16] N. Pisanic, P. R. Randad, K. Kruczynski, Y. C. Manabe, D. L. Thomas, A. Pekosz, S. L. Klein, M. J.
39 Betenbaugh, W. A. Clarke, O. Laeyendecker, *Journal of clinical microbiology* **2020**, 59, e02204.
- 40 [17] a) A. Petherick, *The Lancet* **2020**, 395, 1101; b) D. Li, J. Li, *Journal of clinical microbiology* **2020**,
41 59, e02160.
- 42 [18] T. Gilboa, L. Cohen, C.-A. Cheng, R. Lazarovits, A. Uwamanzu-Nna, I. Han, K. Griswold, N. Barry,
43 D. B. Thompson, R. E. Kohman, *Angewandte Chemie* **2021**.
- 44 [19] K. Quinn, *IPEC-Americas, webinar July 22, 2020*, DOI: [https://ipeamericas.org/excipient-](https://ipeamericas.org/excipient-learning-lab/webinars/novel-ornot-our-inadvertent-journey-filing-novel-excipient)
45 [learning-lab/webinars/novel-ornot-our-inadvertent-journey-filing-novel-excipient](https://ipeamericas.org/excipient-learning-lab/webinars/novel-ornot-our-inadvertent-journey-filing-novel-excipient).

- 1 [20] a) P. B. Gilbert, D. C. Montefiori, A. B. McDermott, Y. Fong, D. Benkeser, W. Deng, H. Zhou, C. R.
2 Houchens, K. Martins, L. Jayashankar, *Science* **2021**, eab3435; b) S. S. DeRoo, N. J. Pudalov, L. Y.
3 Fu, *Jama* **2020**, 323, 2458.
- 4 [21] a) A. Hamady, J. Lee, Z. A. Loboda, *Infection* **2021**, 1; b) N. Eliakim-Raz, Y. Leibovici-Weisman, A.
5 Stemmer, A. Ness, M. Awwad, N. Ghantous, S. M. Stemmer, *Jama* **2021**.
6